RSC Advances

PAPER

View Article Online
View Journal | View Issue

Cite this: *RSC Adv.*, 2020, **10**, 15221

PVP-coated Sb_2Se_3 nanorods as nanotheranostic agents for photoacoustic imaging and photothermal therapy in NIR-I bio-windows†

Botao Qu, ‡[a] Xiaoyan Li,‡[a] Xiaomin Zhang,[a] Weihua Li[b] and Ruiping Zhang*[a]

Received 20th February 2020
Accepted 7th April 2020

DOI: 10.1039/d0ra01638a

rsc.li/rsc-advances

Antimony selenide (Sb_2Se_3) as a simple, low toxicity, low-cost p-type semiconductor material with broad absorbance ranging from the UV to the NIR region has many potential applications in photovoltaic, thermoelectric, and phase-change memory devices. Owing to these excellent properties, Sb_2Se_3 nanorods were firstly synthesized with triphenylantimony and dibenzyldiselenide under solvothermal conditions. In order to enhance the biocompatibility of the Sb_2Se_3 nanorods, polyvinylpyrrolidone (PVP) was coated onto the surface of the Sb_2Se_3 nanorods to form PVP-coated Sb_2Se_3 nanorods. The cell viability of PVP-coated Sb_2Se_3 nanorods toward Hep-2 cells was assessed for 24 h using a Cell Counting Kit-8 (CCK-8) assay. The results showed that Hep-2 cells treated with PVP-coated Sb_2Se_3 nanorods were alive at a concentration as high as 100 μg mL^{-1} in the absence of NIR irradiation. *In vivo* assessment confirmed that PVP-coated Sb_2Se_3 nanorods exhibited excellent photoacoustic imaging and PTT performance, which yielded complete ablation of tumors after laser irradiation (808 nm or 980 nm) in the NIR-I bio-window.

1 Introduction

Semiconductor nanotherapeutics have attracted widespread attention in the treatment of cancer due to their remarkable physicochemical and biochemical properties, such as low band gap, prolonged circulation time and enhanced permeability and retention (EPR) effect.[1–5] Currently, diverse types of nanotherapeutics, such as organic dye ICG; inorganic nanoparticles Pd, Ge, Au, black phosphorus QDs, CuS, MoS_2, Bi_2S_3 and WO_{3-X} nanocrystals; organic semiconducting polymer nanoparticles (SPNs) and ppy nanoparticles, have been investigated for NIR PTT.[6–20] Antimony selenide (Sb_2Se_3) as a simple, low toxicity, low-cost p-type semiconductor material with broad absorbance ranging from the UV to the NIR region has many potential applications in photovoltaic, thermoelectric, and phase-change memory devices.[21–23] Owing to these excellent properties, much effort has been devoted to the fabrication of Sb_2Se_3 and its photovoltaic applications, rarely have this material been explored for its biomedical applications. In view of the above consideration, it is highly recommended to develop a novel Sb_2Se_3 nanotherapeutic agent that can be applied in PTT for cancer cells.

Photothermal therapy (PTT), as a flourishing therapeutic modality, employs light-absorbing agents to generate localized heat upon continuous irradiation of near-infrared (NIR) laser for hyperthermia ablation of cancer cells. In the light of the superiority of PTT in therapeutic modality, such as minimal invasiveness, noninvasive penetration and low toxicity, PTT has received increasing attention in recent years.[24–35] Photoacoustic imaging (PAI), which convert incident light into acoustic waves by exciting nanoparticle or chromophore with a strong optical absorbance spectrum in the NIR region, show powerful advantage such as deep tissue penetration, high spatial resolution, high signal-noise ratio in contrast to conventional X-ray computed tomography (CT), positron emission tomography (PET), magnetic resonance imaging (MRI) and fluorescence images (FLI).[36–49]

In this work, we report a biocompatible PVP-coated Sb_2Se_3 nanorods as PTT theranostic agents with relatively narrow band gap energy, which are responsive to the light (808 and 980 nm) in the NIR-I bio-windows (Scheme 1). The PTT studies *in vitro* and *in vivo* showed that PVP-coated Sb_2Se_3 nanorods were effective for photoacoustic imaging and photothermal destruction of cancer cell. Therefore, Sb_2Se_3 is a promising nanotherapeutics agent for PAI and PTT.

2 Experimental section

2.1 Chemicals

Triphenylantimony (97%), dibenzyldiselenide (98%), PVP-K30 were purchased from Sinopharm Chemicals. Cell Counting Kit (CCK-8) and 4′,6-diamidino-2-phenylindole (DAPI) were

[a]*School of Basic Medical Sciences, Shanxi Medical University, Imaging College of Shanxi Medical University, Imaging Department of the Affiliated Da Yi Hospital of Shanxi Medical University, Taiyuan 030001, Shanxi, China. E-mail: zrp_7142@163.com*

[b]*Department of Radiology, The First Affiliated Hospital of Shenzhen University, Shenzhen Second People's Hospital, Shenzhen 518035, Guangdong, China*

† Electronic supplementary information (ESI) available. See DOI: 10.1039/d0ra01638a

‡ The first two authors contributed equally to this work.

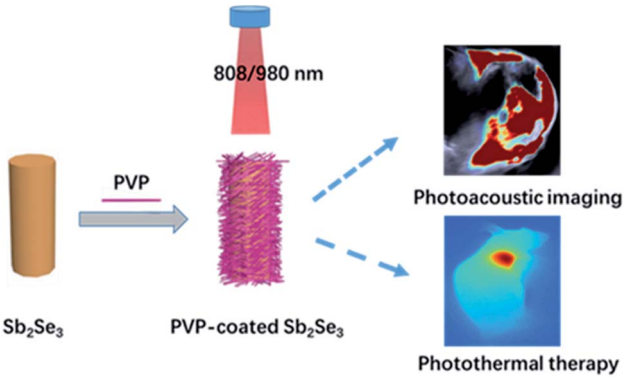

Scheme 1 Schematic illustration of PVP-coated Sb_2Se_3 nanorods nanotheranostic agent for photoacoustic imaging diagnosis and photothermal cancer treatment in NIR-I bio-windows.

purchased from Sigma-Aldrich. All solvents were of analytical grade and used without further purification. Deionized water (18 MΩ cm) used in the experiments was produced from a Milli-Q Gradient System.

2.2 Synthesis of PVP-coated Sb_2Se_3 nanorods

In a typical procedure,[50–52] 0.10 mmol (105.4 mg) triphenylantimony and 0.15 mmol (68 mg) dibenzyldiselenide were dissolved in 5.0 mL oleylamine. Besides, 0.2 g PVP was dissolved in 10 mL EtOH. Then, two solutions were mixed and stirred, transferred into 25 mL Teflon-lined stainless steel autoclave. The reaction was kept at 200 °C for 16 h. After that, the autoclaves were cooled to room temperature naturally. The resulting product was washed with ethanol several times. To improve the biocompatibility of the Sb_2Se_3 nanorods, 10 mg of PVP was dissolved in 2 mL of Sb_2Se_3 nanorods aqueous solution (2 mg mL^{-1}) with stirring for 12 h. After several washes with deionized water, the final product was stored at room temperature for later use.

2.3 CCK-8 assays in laryngeal cancer

Hep-2 cells (≈10 000 cells per well) pressed in a 96-well plate were cultured in fresh media that contained 10% fetal calf serum. The PVP-coated Sb_2Se_3 nanorods at various concentrations were added and cultivated at 37 °C for 24 h. Then, 10 μL of CCK-8 was added to each well after 24 h. The Hep-2 cells were further incubated for 2 h. The determination was carried at 460 nm with enzymatic marker.

2.4 Cell photothermal performance

The photothermal behavior of PVP-coated Sb_2Se_3 nanorods against Hep-2 cells was investigated in the presence or absence of NIR irradiation. Hep-2 cells were seeded at a concentration of 1×10^4 cells per well onto a 96-well plate and precultured for 24 h at 37 °C. After incubated with PVP-coated Sb_2Se_3 nanorods, the cells were exposed to NIR laser (808/980 nm, 1 W cm^{-2}) for 5 min and then stained with calcein AM and PI for 20 min to verify the photothermal behavior for killing cancer cells, and the cells image were obtained using a fluorescence microscope (Olympus, IX73).

2.5 Animal tumor model

The animal procedures were performed in accordance with the Guidelines for Care and Use of Laboratory Animals of Shanxi Medical University, and the experiments were approved by the Animal Ethics Committee of Shanxi Medical University. The six-week-old female nude mice (16–18 g) were purchased from Beijing Vital River Experimental Animal Company. After 2 weeks of acclimatization, tumor models were established by subcutaneous injection of 1×10^6 Hep-2 cells into the RL region of the nude mice. When the tumor volumes reached 100 mm^3, the mice were used for imaging and treatment *in vivo*.

2.6 *In vivo* PAI study

For *in vivo* PAI, the tumor-bearing mice were injected with PVP-coated Sb_2Se_3 nanorods *via* intratumoral administration and then monitored by a real-time MSOT imaging system with a laser wavelength of 730 nm at 1, 2, 4, 6 and 12 h post injection.

2.7 *In vivo* PTT study

To investigate the PTT effect of PVP-coated Sb_2Se_3 nanorods *in vivo*, Hep-2 tumor-bearing mice were divided into four groups and given following treatments: (I), laser (808 nm); (II), PVP-coated Sb_2Se_3 nanorods + laser (808 nm); (III), laser (980 nm); (IV), PVP-coated Sb_2Se_3 nanorods + laser (980 nm). After 2 h intratumoral injection, the mice were irradiated with NIR laser for 5 min. Then an infrared thermal camera (Fluke Ti400) was applied to record the temperature of tumor site. After treatment, the tumor volume and body weight of each mice were inspected in the following 14 days.

2.8 Characterization

The morphology and size of PVP-coated Sb_2Se_3 nanorods were characterized by a TEM (JEOL-2100F) operated at 200 kV. UV-Vis-NIR absorption spectra were acquired by a UV-2550 spectrophotometer. The Fourier transform infrared (FTIR) spectrum was measured by a Vector 22 spectrometer with KBr pellets (Bruker AXS, Inc., Madison, WI, USA). Thermogravimetric analyses (TGA) were performed on a simultaneous SDT 2960 thermal analyzer from 30 to 600 °C with a heating rate of 20 °C min^{-1} under N_2 atmosphere. Zeta potential were measured by a Nano-Zetasizer (Malvern Instruments Ltd.).

3 Results and discussion

Sb_2Se_3 nanorods were prepared using a previously reported method with slight modification. PVP was coated on the surface of Sb_2Se_3 nanorods in order to enhance the biocompatibility of Sb_2Se_3 nanorods. The successful coating of the Sb_2Se_3 nanorods can be verified by the TGA (Fig. 1C) and FT-IR spectra (Fig. S1†). Thermogravimetric analysis revealed that the mass fraction of PVP in the as-prepared PVP-coated Sb_2Se_3 nanorods is 7%.[53] The characteristic absorption band at 1660 cm^{-1} belongs to the

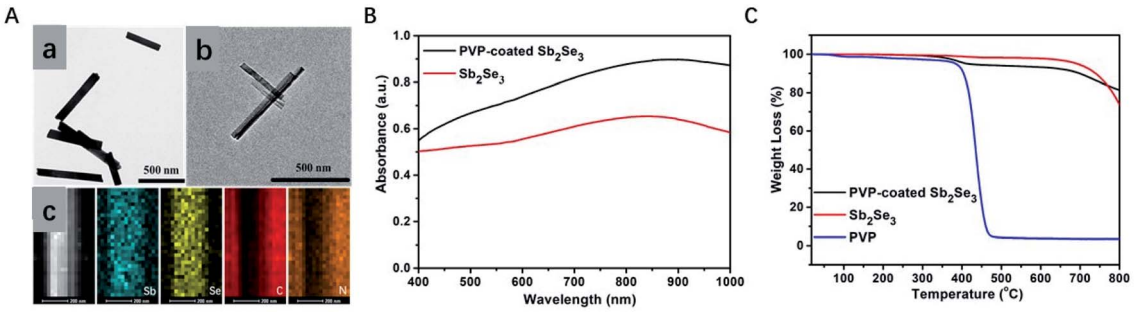

Fig. 1 TEM images of Sb_2Se_3 (A-a) and PVP-coated Sb_2Se_3 nanorods (A-b) and (A-c) EDX elemental mapping images of PVP-coated Sb_2Se_3 nanorods. (B) UV-vis-NIR absorption spectra of Sb_2Se_3 and PVP-coated Sb_2Se_3 nanorods aqueous solution. (C) TGA curves of PVP, Sb_2Se_3 and PVP-coated Sb_2Se_3 nanorods.

C═O stretching vibration mode, suggesting that the coating of PVP on the surface Sb_2Se_3.[54] Due to the low loading capacity, the FT-IR spectra of PVP-coated Sb_2Se_3 nanorods show weak absorbance intensity. Transmission electron microscopy (TEM) images of Sb_2Se_3 and PVP-coated Sb_2Se_3 nanorods were shown in Fig. 1A. All the PVP-coated Sb_2Se_3 show a nanorod morphology with average size of 500 nm. The composition of the core–shell nanostructures was more evident from the EDX elemental mapping data. Evidently, the elements Sb and Se is mainly distributed in the core and the elements C and N are homogenously distributed throughout the whole nanostructures, indicating that the Sb_2Se_3 core is surrounded with a uniform and continuous PVP shell. The ζ potentials of Sb_2Se_3 and PVP-coated Sb_2Se_3 nanorods are −20 mV and +2.5 mV, respectively (Fig. S2†). All data above indicate that the layer coated on Sb_2Se_3 nanorods is PVP. UV-Vis spectra were recorded to investigate the effect of Sb_2Se_3 and PVP-coated Sb_2Se_3 nanorods. As displayed in Fig. 1B, the Sb_2Se_3 and PVP-coated Sb_2Se_3 nanorods show similar absorbance spectra from 400 to 1000 nm. However, the absorbance of PVP-coated Sb_2Se_3 nanorods is much higher than Sb_2Se_3 in the range of 400 to 1000 nm, which encourage us to further explore the PA performance of PVP-coated Sb_2Se_3 nanorods. To evaluate photoacoustic behavior of PVP-coated Sb_2Se_3 nanorods, the photoacoustic signals of PVP-coated Sb_2Se_3 nanorods aqueous dispersions with concentrations from 0.2 to 1.0 mg mL^{-1} were determined with water. As shown in Fig. 4C, PVP-coated Sb_2Se_3 nanorods aqueous solution showed concentration-dependent PA signals under 808 nm light excitation due to their

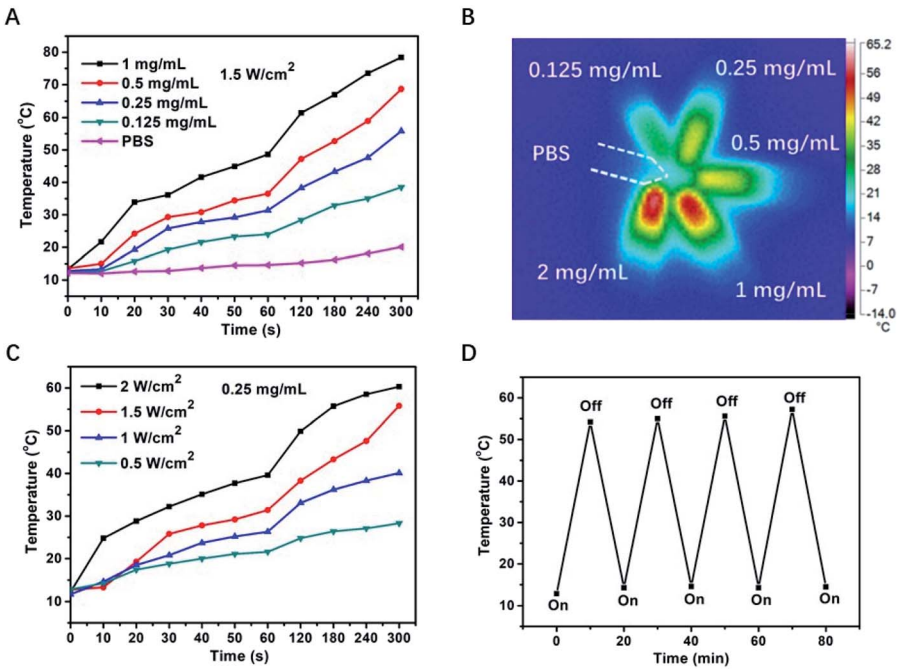

Fig. 2 (A) Temperature changes of PVP-coated Sb_2Se_3 nanorods at different concentrations exposed to 808 nm laser at a power density of 1.5 W cm^{-2}. (B) Infrared thermal images of the solution containing PVP-coated Sb_2Se_3 nanorods under the NIR laser (808 nm, 1.0 W cm^{-2}) irradiation for 5 min. (C) Temperature change of PVP-coated Sb_2Se_3 nanorods at a constant concentration with different power. (D) Temperature variation of PVP-coated Sb_2Se_3 nanorods aqueous solution under 808 nm laser irradiation (1.0 W cm^{-2}) for four laser on/off cycles.

thermoelastic expansion in aqueous solution, indicating that PVP-coated Sb_2Se_3 nanorods might act as a PA contrast agent.

In order to investigate the photothermal properties of the obtained PVP-coated Sb_2Se_3 nanorods, PVP-coated Sb_2Se_3 nanorods with different concentrations (0, 0.125, 0.25, 0.5 and 1.0 mg mL^{-1}) were irradiated with an 808 nm laser for 300 s. The temperature elevation of PVP-coated Sb_2Se_3 nanorods aqueous dispersions shows an obvious concentration-dependent temperature increase in response to NIR irradiation (808 nm, 1.5 W cm^{-2}) (Fig. 2A), especially for that with a higher PVP-coated Sb_2Se_3 nanorods concentration and extended irradiation duration. For example, the temperature of PVP-coated Sb_2Se_3 nanorods (0.25 mg mL^{-1}) raised up to 55 °C within 5 min which can kill cancer cells effectively, while the control group of phosphate buffered saline (PBS) only showed a mild temperature elevation (from 12.2 to 20.0 °C). The color change in the photothermal images was clearly observed (Fig. 2B), which was measured using an infrared thermal camera with the PVP-coated Sb_2Se_3 nanorods solution (0.125, 0.25, 0.5, 1.0 and 2.0 mg mL^{-1}) under 808 nm light exposure at 1.0 W cm^{-2} for 5 min and PBS was selected as the control. It is clearly seen that the photothermal effect of PVP-coated Sb_2Se_3 nanorods was proportionally improved as the concentrations increased. At the same concentration of 0.25 mg mL^{-1}, the

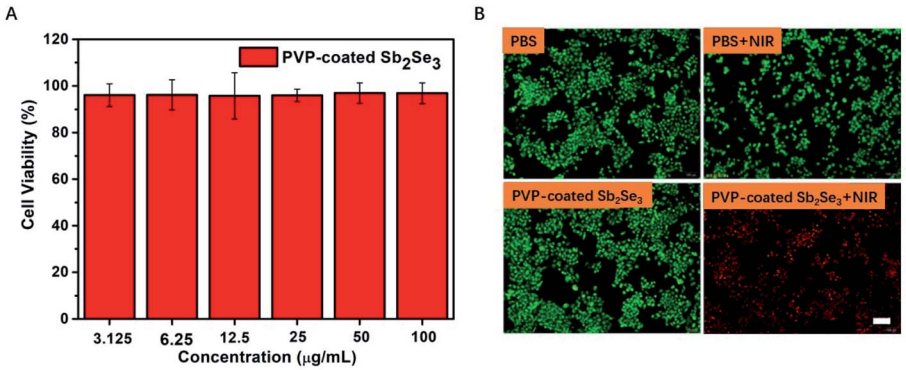

Fig. 3 (A) Cell viability of Hep-2 cells after cultured with various concentrations of PVP-coated Sb_2Se_3 nanorods for 24 h. (B) Fluorescence images of live (green) and dead (red) cells stained by calcein AM and PI after being treated with PBS, PBS + NIR (808 nm), PVP-coated Sb_2Se_3 nanorods, and PVP-coated Sb_2Se_3 nanorods + NIR (808 nm). Scale bar: 100 μm.

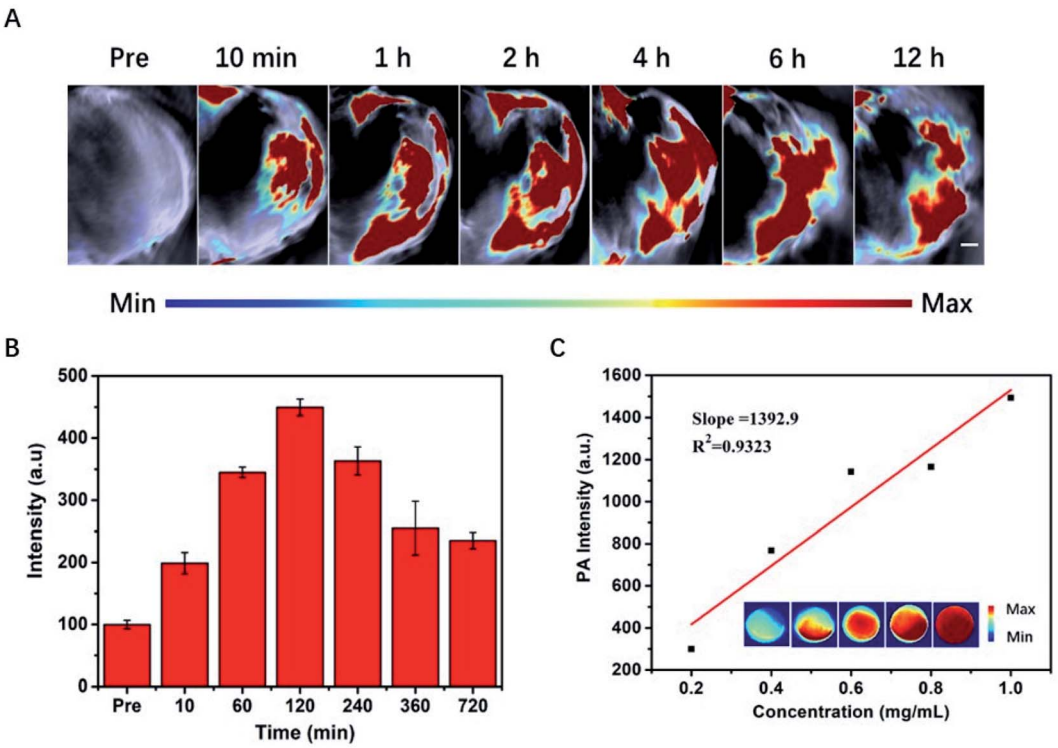

Fig. 4 (A) PA images of tumors at different time points after injection of PVP-coated Sb_2Se_3 nanorods. (B) Quantitative analysis of PA values in (A). (C) Linear relationship between concentrations and PA signals, with corresponding PA images in the inset.

temperature increase of the PVP-coated Sb_2Se_3 nanorods solution may be controlled under continuous radiation of an 808 nm laser, as shown in Fig. 2C. It also confirmed that the photothermal effect of the PVP-coated Sb_2Se_3 nanorods solution was complying with a laser power density-dependent mode.

To evaluate their photostability, four cycles of light irradiation was carried out (Fig. 2D). PVP-coated Sb_2Se_3 nanorods dispersions (0.5 mg mL^{-1}) was irradiated with 808 nm laser at 1 W cm^{-2} for 10 min, and the irradiation was tuned off for leaving the photothermal temperature to room temperature. The same switch on/off was repeated for another three times. The results exhibited that PVP-coated Sb_2Se_3 nanorods showed the temperature increase of 54.2 °C after the first irradiation, and there was no obvious change in temperature variation after three switch on/off cycles, suggesting that PVP-coated Sb_2Se_3 nanorods dispersions possess excellent photostability under repeated irradiation. The photothermal and photostability behavior of PVP-coated Sb_2Se_3 nanorods upon 980 nm laser irradiation was also investigated, similar outcome was shown in Fig. S3,† which attributed to the NIR absorption.

In view of above results, NIR-mediated PVP-coated Sb_2Se_3 nanorods displaying photothermal effect urge us to examine phototherapeutic effect toward Hep-2 cells *in vitro*. Prior to *in vitro* photothermal therapy, the biosafety evaluation illustrated in Fig. 3A is vitally important for the next task. Therefore, the cell viability of PVP-coated Sb_2Se_3 nanorods toward Hep-2 cells was assessed for 24 h by Cell Counting Kit-8 (CCK-8) assay. The result showed that Hep-2 cells treated with PVP-coated Sb_2Se_3 nanorods were alive at a concentration as high as 100 μg mL^{-1} in the absence of NIR irradiation. Furthermore, a live/dead cell assay was performed using calcein acetoxymethyl (calcein AM, green) and propidium iodide (PI, red) staining after NIR light irradiation at 808 nm for 5 min. Under NIR light irradiation, almost all the cells induced by PVP-coated Sb_2Se_3 nanorods to death emitted red fluorescence. In contrast, there was green fluorescence observed in the absence of laser irradiation, which implied that cells were living (Fig. 3B and S4†). In a word, these results indicate that PVP-coated Sb_2Se_3 nanorods have promising potential as a photothermal agent to kill cancer cells. We further investigate photothermal effect and live/dead cell assay of PVP-coated Sb_2Se_3 nanorods under 980 nm laser irradiation, as shown in Fig. S5.† All results confirmed that PVP-coated Sb_2Se_3 nanorods show promising photothermal ability for killing cancer cells in the NIR-I bio-windows.

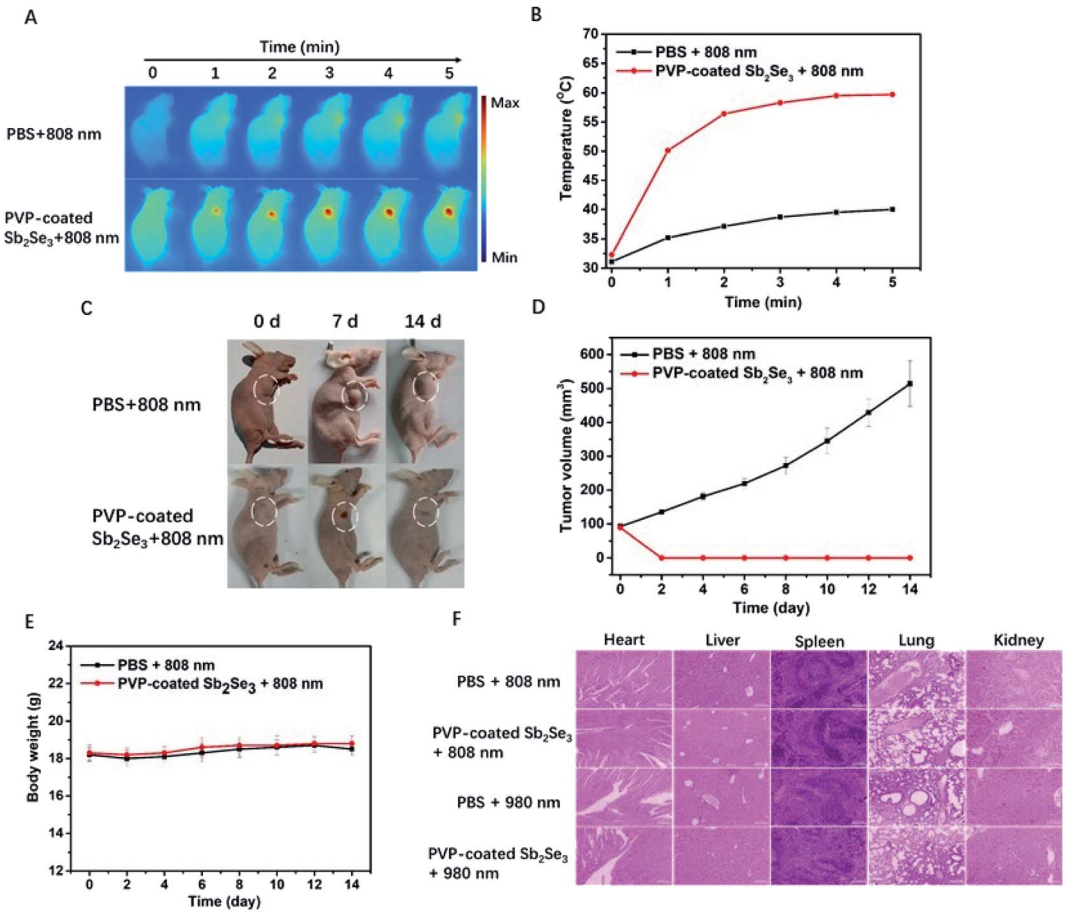

Fig. 5 (A) IR thermal images of Hep-2 tumor bearing nude mice. (B) Time-dependent temperature change in mice tumor after different treatments. (C) Representative photographs of mice tumor after various treatment 0–14 day. (D) Tumor growth curves of Hep-2 tumor bearing nude mice after treatment for 14 days. (E) Body weights of mice during different treatments. (F) H&E staining images of major organs (heart, liver, spleen, lung, kidney). Scale bar: 100 μm.

Encouraged by the photoacoustic and photothermal properties *in vitro*, we continued to evaluate the potential of PVP-coated Sb_2Se_3 nanorods as photoacoustic imaging and thermal imaging agent. The PA imaging was investigated *in vivo*. As shown in Fig. 4A, mice bearing Hep-2 tumors were injected with PVP-coated Sb_2Se_3 nanorods. PA signals in tumor was gradually enhanced over time and reached their maximum 2 h after injection, indicating that the optimal treatment time was 2 h after i.t. injection (Fig. 4B). Furthermore, the IR thermal imaging was applied to detect the real-time temperature of tumor region at 2 h post injection. For mice treated with PVP-coated Sb_2Se_3 nanorods, tumor temperature gradually increased to 60 °C within 5 min when exposed to 808 nm laser, while the temperature of control group displayed little change (Fig. 5A and B). In comparison, the tumor temperature reaches 57.5 °C exposed to 980 nm laser under the same condition, both of which could absolutely meet to the requirement and efficacy of PTT (Fig. S6A and B†). Thus, the PVP-coated Sb_2Se_3 nanorods could be utilized as photoacoustic and photothermal contrast agent.

In view of above good PAI and PTT, upon NIR light irradiation, we further evaluated the potential application of PVP-coated Sb_2Se_3 nanorods for cancer therapy using the Hep-2 tumor bearing nude mice. At 2 h postinjection, the 808 nm or 980 nm NIR laser was applied to irradiate the tumor site. After 14 d of treatment, the tumor was completely eliminated in the PVP-coated Sb_2Se_3 nanorods plus laser and increased in PBS plus laser (Fig. 5C and S6C†), which is in accordance with the tumor volume change (Fig. 5D and S6D†). More importantly, the body weight of the mice showed no apparent change during treatment (Fig. 5E and S6E†). Due to complete ablation of tumor after treatment, the hematoxylin and eosin (H&E) staining of tumor slides have not been shown. Meanwhile, there were no evident organs damage observed in the slices collected from major organs of control group and PVP-coated Sb_2Se_3 nanorods plus laser, indicating the negligible toxicity of PVP-coated Sb_2Se_3 nanorods *in vivo* (Fig. 5F). The *in vivo* photothermal therapy by i.t. injection further verified the efficient cancer therapy ability of PVP-coated Sb_2Se_3 nanorods.

4 Conclusions

In summary, this work firstly presented the biomedicine application of PVP-coated Sb_2Se_3 nanorods as photothermal nanotherapeutics under either 808 nm or 980 nm in fighting against cancer cell. Due to the strong NIR absorption capability in the NIR-I bio-windows (750–1000 nm),[55] the PVP-coated Sb_2Se_3 nanorods display preferable photoacoustic and photothermal behavior. *In vivo* assessment confirmed that PVP-coated Sb_2Se_3 nanorods effectively induced PTT properties, which yielded complete ablation of tumor after laser irradiation (808 nm or 980 nm) in the NIR-I bio-windows. This work inspires us to develop much more photovoltaic semiconductor materials with low toxicity and expands their potential application in biomedical field for cancer treatment.

Conflicts of interest

There are no conflicts to declare.

Acknowledgements

This work has been financially supported by the National Natural Science Foundation of China (No. 81571747, 81771907), Science and technology innovation team project of Shanxi Province (No. 201705D131026), Engineering Technology Research Center of Shanxi Province (No. 201805D121008) Scientific and technological achievements transformation project of Shanxi Province (No. 201704D131006), Laboratory Construction Project of Shanxi Province, The Projects for Local Science and Technology Development Guided by the Central Committee (YDZX20191400002537), Natural Science Foundation of Shanxi Province (No. 201901D111213) and Startup Foundation for Doctors of Shanxi Medical University (No. 03201505).

Notes and references

1 S. Wang, A. Riedinger, H. Li, C. Fu, H. Liu, L. Li, T. Liu, L. Tan, M. J. Barthel, G. Pugliese, F. De Donato, M. Scotto D'Abbusco, X. Meng, L. Manna, H. Meng and T. Pellegrino, *ACS Nano*, 2015, **9**, 1788–1800.
2 B. Godin, E. Tasciotti, X. Liu, R. E. Serda and M. Ferrari, *Acc. Chem. Res.*, 2011, **44**, 979–989.
3 X. Zhen, C. Xie and K. Pu, *Angew. Chem.*, 2018, **57**, 3938–3942.
4 W. Li, P. Rong, K. Yang, P. Huang, K. Sun and X. Chen, *Biomaterials*, 2015, **45**, 18–26.
5 W. Huang, Y. Huang, Y. You, T. Nie and T. Chen, *Adv. Funct. Mater.*, 2017, **27**, 1701388.
6 M. Zhu, Z. Sheng, Y. Jia, D. Hu, X. Liu, X. Xia, C. Liu, P. Wang, X. Wang and H. Zheng, *ACS Appl. Mater. Interfaces*, 2017, **9**, 39249–39258.
7 C. Zhang, L. Zhou, J. Zhang, Y. Y. Fu, X. Zhang, C. Yu, S. K. Sun and X. P. Yan, *Nanoscale*, 2016, **8**, 16204–16211.
8 Q. Chen, L. Xu, C. Liang, C. Wang, R. Peng and Z. Liu, *Nat. Commun.*, 2016, **7**, 13193.
9 P. Zhao, Z. Jin, Q. Chen, T. Yang, D. Chen, J. Meng, X. Lu, Z. Gu and Q. He, *Nat. Commun.*, 2018, **9**, 4241.
10 W. Sun, G. Zhong, C. Kübel, A. A. Jelle, C. Qian, L. Wang, M. Ebrahimi, L. M. Reyes, A. S. Helmy and G. A. Ozin, *Angew. Chem., Int. Ed.*, 2017, **56**, 6329–6334.
11 W. Shang, C. Zeng, Y. Du, H. Hui, X. Liang, C. Chi, K. Wang, Z. Wang and J. Tian, *Adv. Mater.*, 2017, **29**, 1604381.
12 X. Zhao, C.-X. Yang, L.-G. Chen and X.-P. Yan, *Nat. Commun.*, 2017, **8**, 14998.
13 Z. Sun, H. Xie, S. Tang, X. F. Yu, Z. Guo, J. Shao, H. Zhang, H. Huang, H. Wang and P. K. Chu, *Angew. Chem.*, 2015, **54**, 11526–11530.
14 Q. Tian, M. Tang, Y. Sun, R. Zou, Z. Chen, M. Zhu, S. Yang, J. Wang, J. Wang and J. Hu, *Adv. Mater.*, 2011, **23**, 3542–3547.
15 R. Marin, A. Skripka, L. V. Besteiro, A. Benayas, Z. Wang, A. O. Govorov, P. Canton and F. Vetrone, *Small*, 2018, 1803282.
16 Q. Gao, X. Zhang, W. Yin, D. Ma, C. Xie, L. Zheng, X. Dong, L. Mei, J. Yu, C. Wang, Z. Gu and Y. Zhao, *Small*, 2018, **14**, 1802290.

17 Z. Xiao, C. Xu, X. Jiang, W. Zhang, Y. Peng, R. Zou, X. Huang, Q. Liu, Z. Qin and J. Hu, *Nano Res.*, 2016, **9**, 1934–1947.
18 K. Deng, Z. Hou, X. Deng, P. Yang, C. Li and J. Lin, *Adv. Funct. Mater.*, 2015, **25**, 7280–7290.
19 Y. Jiang, P. K. Upputuri, C. Xie, Y. Lyu, L. Zhang, Q. Xiong, M. Pramanik and K. Pu, *Nano Lett.*, 2017, **17**, 4964–4969.
20 X. Wang, Y. Ma, X. Sheng, Y. Wang and H. Xu, *Nano Lett.*, 2018, **18**, 2217–2225.
21 Y. Zhou, L. Wang, S. Chen, S. Qin, X. Liu, J. Chen, D.-J. Xue, M. Luo, Y. Cao, Y. Cheng, E. H. Sargent and J. Tang, *Nat. Photonics*, 2015, **9**, 409.
22 M. S. Dresselhaus, G. Chen, M. Y. Tang, R. G. Yang, H. Lee, D. Z. Wang, Z. F. Ren, J. P. Fleurial and P. Gogna, *Adv. Mater.*, 2007, **19**, 1043–1053.
23 C. Karthik, R. J. Mehta, W. Jiang, E. Castillo, T. Borca-Tasciuc and G. Ramanath, *Appl. Phys. Lett.*, 2011, **99**, 103101.
24 S. Liang, Z. Xie, Y. Wei, Z. Cheng, Y. Han and J. Lin, *Dalton Trans.*, 2018, **47**, 7916–7924.
25 R. Zhang, K. Cheng, A. L. Antaris, X. Ma, M. Yang, S. Ramakrishnan, G. Liu, A. Lu, H. Dai, M. Tian and Z. Cheng, *Biomaterials*, 2016, **103**, 265–277.
26 W. Wang, L. Wang, Y. Li, S. Liu, Z. Xie and X. Jing, *Adv. Mater.*, 2016, **28**, 9320–9325.
27 Z. Wang, Z. Chang, M. Lu, D. Shao, J. Yue, D. Yang, M. Li and W. F. Dong, *ACS Appl. Mater. Interfaces*, 2017, **9**, 30306–30317.
28 T. T. Zhang, C. H. Xu, W. Zhao, Y. Gu, X. L. Li, J. J. Xu and H. Y. Chen, *Chem. Sci.*, 2018, **9**, 6749–6757.
29 Z. Li, Y. Hu, Z. Miao, H. Xu, C. Li, Y. Zhao, Z. Li, M. Chang, Z. Ma, Y. Sun, F. Besenbacher, P. Huang and M. Yu, *Nano Lett.*, 2018, **18**, 6778–6788.
30 K. Zhang, X. Meng, Y. Cao, Z. Yang, H. Dong, Y. Zhang, H. Lu, Z. Shi and X. Zhang, *Adv. Funct. Mater.*, 2018, **28**, 1804634.
31 L. Song, X. Dong, S. Zhu, C. Zhang, W. Yin, X. Zhang, X. Liu and Z. Gu, *Adv. Healthcare Mater.*, 2018, **7**, 1800830.
32 X. Ji, N. Kong, J. Wang, W. Li, Y. Xiao, S. T. Gan, Y. Zhang, Y. Li, X. Song, Q. Xiong, S. Shi, Z. Li, W. Tao, H. Zhang, L. Mei and J. Shi, *Adv. Mater.*, 2018, **30**, 1803031.
33 J.-Y. Zeng, M.-K. Zhang, M.-Y. Peng, D. Gong and X.-Z. Zhang, *Adv. Funct. Mater.*, 2017, **28**, 1705451.
34 S. Wang, X. Ma, X. Hong, Y. Cheng, Y. Tian, S. Zhao, W. Liu, Y. Tang, R. Zhao, L. Song, Z. Teng and G. Lu, *ACS Nano*, 2018, **12**, 662–670.
35 S. Goel, C. A. Ferreira, F. Chen, P. A. Ellison, C. M. Siamof, T. E. Barnhart and W. Cai, *Adv. Mater.*, 2018, **30**, 1704367.
36 R. Zhang, Q. Fan, M. Yang, K. Cheng, X. Lu, L. Zhang, W. Huang and Z. Cheng, *Adv. Mater.*, 2015, **27**, 5063–5069.
37 Q. Fan, K. Cheng, X. Hu, X. Ma, R. Zhang, M. Yang, X. Lu, L. Xing, W. Huang, S. S. Gambhir and Z. Cheng, *J. Am. Chem. Soc.*, 2014, **136**, 15185–15194.
38 M. Yang, Q. Fan, R. Zhang, K. Cheng, J. Yan, D. Pan, X. Ma, A. Lu and Z. Cheng, *Biomaterials*, 2015, **69**, 30–37.
39 J. Sun, W. Xu, L. Li, B. Fan, X. Peng, B. Qu, L. Wang, T. Li, S. Li and R. Zhang, *Nanoscale*, 2018, **10**, 10584–10595.
40 X. Jiang, S. Zhang, F. Ren, L. Chen, J. Zeng, M. Zhu, Z. Cheng, M. Gao and Z. Li, *ACS Nano*, 2017, **11**, 5633–5645.
41 P. Si, E. Yuan, O. Liba, Y. Winetraub, S. Yousefi, E. D. SoRelle, D. W. Yecies, R. Dutta and A. de la Zerda, *ACS Nano*, 2018, **12**, 11986–11994.
42 Q. Zou, J. Huang and X. Zhang, *Small*, 2018, **14**, 1803101.
43 P. Garrigue, J. Tang, L. Ding, A. Bouhlel, A. Tintaru, E. Laurini, Y. Huang, Z. Lyu, M. Zhang, S. Fernandez, L. Balasse, W. Lan, E. Mas, D. Marson, Y. Weng, X. Liu, S. Giorgio, J. Iovanna, S. Pricl, B. Guillet and L. Peng, *Proc. Natl. Acad. Sci. U. S. A.*, 2018, **115**, 11454–11459.
44 Q. Jin, W. Zhu, D. Jiang, R. Zhang, C. J. Kutyreff, J. W. Engle, P. Huang, W. Cai, Z. Liu and L. Cheng, *Nanoscale*, 2017, **9**, 12609–12617.
45 J. C. Yang, Y. Chen, Y. H. Li and X. B. Yin, *ACS Appl. Mater. Interfaces*, 2017, **9**, 22278–22288.
46 Z. Shen, T. Liu, Y. Li, J. Lau, Z. Yang, W. Fan, Z. Zhou, C. Shi, C. Ke, V. I. Bregadze, S. K. Mandal, Y. Liu, Z. Li, T. Xue, G. Zhu, J. Munasinghe, G. Niu, A. Wu and X. Chen, *ACS Nano*, 2018, **12**, 11355–11365.
47 H. Wan, H. Ma, S. Zhu, F. Wang, Y. Tian, R. Ma, Q. Yang, Z. Hu, T. Zhu, W. Wang, Z. Ma, M. Zhang, Y. Zhong, H. Sun, Y. Liang and H. Dai, *Adv. Funct. Mater.*, 2018, 1804956.
48 J. S. Ni, P. Zhang, T. Jiang, Y. Chen, H. Su, D. Wang, Z. Q. Yu, R. T. K. Kwok, Z. Zhao, J. W. Y. Lam and B. Z. Tang, *Adv. Mater.*, 2018, 1805220.
49 X. Hao, C. Li, Y. Zhang, H. Wang, G. Chen, M. Wang and Q. Wang, *Adv. Mater.*, 2018, 1804437.
50 G. Chen, J. Zhou, J. Zuo and Q. Yang, *ACS Appl. Mater. Interfaces*, 2016, **8**, 2819–2825.
51 R. J. Mehta, C. Karthik, W. Jiang, B. Singh, Y. Shi, R. W. Siegel, T. Borca-Tasciuc and G. Ramanath, *Nano Lett.*, 2010, **10**, 4417–4422.
52 J. Ma, Y. Wang, Y. Wang, P. Peng, J. Lian, X. Duan, Z. Liu, X. Liu, Q. Chen, T. Kim, G. Yao and W. Zheng, *CrystEngComm*, 2011, **13**, 2369–2374.
53 P. Lei, R. An, P. Zhang, S. Yao, S. Song, L. Dong, X. Xu, K. Du, J. Feng and H. Zhang, *Adv. Funct. Mater.*, 2017, **27**, 1702018.
54 J. Wei, J. Li, D. Sun, Q. Li, J. Ma, X. Chen, X. Zhu and N. Zheng, *Adv. Funct. Mater.*, 2018, **28**, 1706310.
55 H. Lin, S. Gao, C. Dai, Y. Chen and J. Shi, *J. Am. Chem. Soc.*, 2017, **139**, 16235–16247.